A network of chemical reactions for modeling hydrocracking reactors
Proceedings of European Congress of Chemical Engineering (ECCE-6)
Copenhagen, 16-20 September 2007

A network of chemical reactions for modeling hydrocracking reactors

R.M.C. Ferreira da Silva[a], J.L. de Medeiros[b], O.Q.F. Araújo[b]

[a]*CENPES, PETROBRAS, Ilha do Fundão 21949-900, Rio de Janeiro, RJ, Brazil*
[b]*Escola de Quimica, Universidade Federal do Rio de Janeiro, 21949-900, Rio de Janeiro, RJ, Brazil*

Abstract

We studied some of the phases involved in the development of a HCC reactor model within a molecular-structure-based approach. Phase 1 considers a chemical description of HCC feeds. We use a discrete compositional model for a pre-hydrotreated heavy vacuum gasoil which constitutes a typical feed of a hydrocracking bed in the second stage of a HCC process. A set of hydrocarbon families is formulated to cover relevant functional molecular sub-structures quantifiable by analytical procedures of feedstocks and products. Each family has parameters defining its concentration and mean molecular weight distribution, and is complemented by a framework of rules for generation of molecular structures belonging to it. Feed parameters were estimated by reconciliation of property predictions with available characterizing data. Phase 2 is concerned with the HCC reactions network and the corresponding kinetic mechanisms. Empirical kinetic rules from the Literature were applied for proposing a HCC reaction network adopting molecule-based kinetics. Reactions rates were modeled according to several mechanisms involving gas-liquid equilibrium and adsorption equilibrium along an experimental isothermal reactor. In order to keep the model within tractable limits, kinetic and adsorption parameters were grouped into a primary and a secondary sets. The secondary set is calculated from the primary set via empirical proportionality factors. The primary set was estimated via non-linear regression of predicted properties over data of HCC products

Keywords: hydrocracking, HCC, compositional model, molecular-based kinetics

1. Introduction

The current petroleum market exhibits a trend of gradual increase in the participation of low quality crudes characterized by high carbon/hydrogen ratios and high contents of sulphur/nitrogen/polyaromatics. The processing of such crudes leads to high yields of heavy fractions in detriment of middle distillates. In this scenario, the Technology of Hydrocracking (HCC) can guarantee stringent specified urban fuels by providing qualitative upgrading of heavy fractions via increase of their hydrogen/carbon ratio as

well by eliminating contaminant heteroatoms and enhancing yields of naphtha and middle fractions. HCC is a severe reactive process characterized by massive hydrogenation of hydrocarbon molecules where aromatic hydrogenation, paraffin cracking, isomerization, dealkylation and naphthenic ring opening take place. All products of HCC processes are completely free of heteroatoms (S or N) because the HCC feed must be profoundly hydrotreated previously. HCC technology is, on the other hand, costly because it demands high usage of hydrogen at extremely severe reactor conditions (temperature, pressure and spatial time). Thus, it is not surprising that HCC plants are rare in the refinery context around the world.

Inherently connected to this, modeling studies of HCC are also scarce. Plausible reasons derive from a large set of theoretical obstacles that characterize HCC like: (i) complex (true) chemical description of HCC feeds; (ii) complex chain of chemical transformations involved and associated chemical reaction network; (iii) complex behavior of reaction rates; and (iv) complex hydrodynamic, kinetic and thermal effects through the reactor.

HCC processes are designed for heavy feeds like heavy vacuum gasoils (HVGO) which must previously pass through a Hydrotreatment (HDT) reactor. The effluent from the HDT stage is a complex mixture with several hundreds of distinct hydrocarbon species with practically no heteroatoms. As the mixture flows through the HCC bed, it is plausible that thousands of other compounds are created and destroyed during the complex chain of transformations inside the reactor. Accurate description of the behavior of such mixtures is important to the design and operation of HCC processes, but it configures a formidable challenge to identify, according to an organized fashion, the myriad of compounds and establish the connectivity between them through a complex HCC digraph of catalytic chemical reactions. So it is no surprise that HCC models invariably resort to aggregation procedures like molecular and reaction lumping.

A scheme of a HCC plant for processing heavy vacuum gasoil (HVGO) is shown in Fig. 1. After receiving the addition of recycled H_2, the HVGO is heated in exchanger (P-01), heater (F-01), and fed to reactor R-01 for the First Stage of reaction, designed for adjusting organic nitrogen/sulfur to levels tolerated by the HCC catalyst, by conversion to NH_3/H_2S. In R-01 HVGO is pre-hydrotreated with a conventional HDT catalyst (alumina loaded with NiO/MoO_3). After gas-liquid split in drum V-02, the product of R-01 is mixed with fresh H_2, heated in exchanger P-02 and heater F-02, and then flows to the Second Stage of reaction, passing first through reactor R-02 to resume the HDT. The liquid effluent of R-02 is the hydrotreated heavy vacuum gasoil (H-HVGO) which goes finally to R-03 for HCC. The beds of R-03 are loaded with bifunctional catalyst (amorphous acid support or zeolite with metallic components). Temperature control of R-01/R-02/R-03 is accomplished via intermediate injection of recycle gas. The effluent of R-03 is cooled (P-02/P-03) and sent to separator (V-03), where NH_3/H_2S are absorbed in water. The separated hydrocarbon liquid is fractioned in tower T-01 to several products like kerosene, naphtha and diesel. The gas rich in H_2, after compressed by the recycle compressor (C-01), is reused in various sites of the unit.

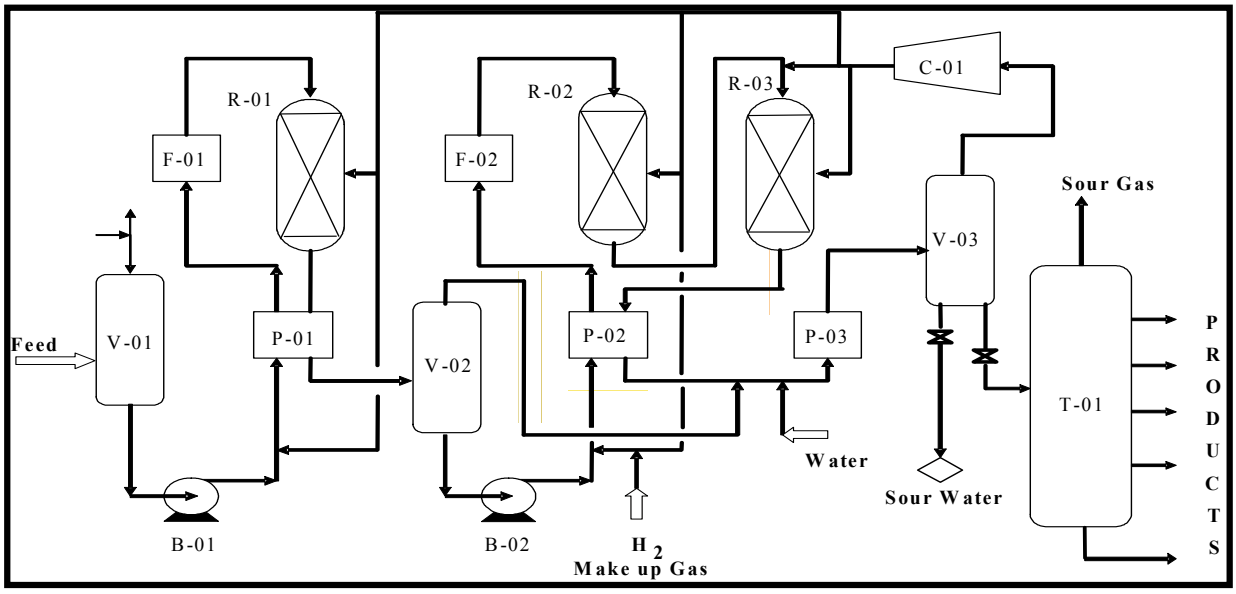

Figure 1 : Simplified Flowsheet for Hydrocracking Heavy Vacuum Gasoil

Consistent with analytical limitations, early HCC models have implemented lumping approaches with a relatively small number of lumps to describe the mixture and the subsequent chemical transformations (Raychaudhuri et al, 1994). In this implementation the several hundreds of individual constituents of a complex feedstock are grouped into a few (but measurable) categories of boiling range. These categories define the lumps. Connecting the lumps, simplified HCC reaction pathways are established. The rate of conversion of mass from one lump to another is supposed to follow a kinetic model depending on the concentration of lumps and on appropriate temperature dependent kinetic coefficients.

HCC processes convert heavy feedstocks to middle and light distillates. Thus, every conversion of mass from a higher molecular weight lump to a lighter one must be taken into account. Although satisfying the needs of HCC designers in the past, the classical lumping has several inherent limitations that have been discussed extensively in the literature (Quann and Jaffe, 1996; Basak et al., 2004), namely: (1) molecular information is obscured by the multicomponent nature of lumps, precluding the use of precise thermodynamic models for property prediction; (2) the approach fails to extrapolate to different feedstocks due to composition differences within the same defined lumps; i.e. the rate coefficients obtained are feed sensitive and must be determined for each feedstock/catalyst combination; (3) the actual composition of lumps may change with overall conversion, thus masking true kinetics; (4) lumped models cannot be used to interpret the effects of catalyst properties on the phenomenology of the reaction because fundamental catalysis mechanisms are not incorporated into the lump scheme; and (5) another obstacle appears if the final aim is to attain not only optimal product yield but also market quality specifications, because the lack of true molecular information in the lumping context complicates accurate prediction of product properties.

In the last two decades, kinetics models based on reaction mechanism and elementary steps have been developed for HCC and catalytic cracking. One successful method of this class is the single-event kinetic approach that has found applications in hydrocracking and hydro-isomerization (Svoboda et al, 1995). The single-event approach depends on the chemical knowledge of the elementary chemical steps occurring on catalyst surface, retaining the detail of the reaction network and taking into account several kinetic rules. The hundreds of rate coefficients of the elementary steps in the reaction network are expressed in terms of a large number of single-event rate coefficients. Due to its fundamental nature, the single-event model requires a molecular analysis of the feedstock, entailing that a certain degree of lumping is unavoidable in practical applications. Although theoretically independent of feedstock or reactor configuration, the application of single-event models to industrial processes is still far from being achieved due to analytical complexity and modeling limitations.

Increasing environment concerns have focused attention on composition aspects of heavy feedstocks and products. These recent trends and also analytical/computational progresses motivate the development of molecule-based fundamental kinetic models for simulation and optimization of refinery processes. In this context, a method called Structure Oriented Lumping – SOL, was proposed for different reactive applications (Quann and Jaffe, 1996). The basic concept involves a formal, recursive, description of hydrocarbon molecules as vectors of structural characteristic elements sufficient to construct any molecule. As can be expected, SOL methodology must be complemented by group contribution property prediction frameworks (Reid et al., 1987). More than a way of formal enumeration of molecular structures, the SOL descriptor enables also a formal way to address the tree of molecules that can be created from a given species via a characteristic reactive process like hydrogenation. Since the SOL method aims to describe the true molecular collective that is relevant to a reactive application, an apparent disadvantage is the impacting large number of species and reactions that have to be formulated in a typical HCC application.

The impressive number of different hydrocarbon species belonging to the scenario of HCC of gasoils, together with the quasi-continuity that characterizes the space of pertinent species, suggests strongly the application of a mathematical limit known as Continuous Lumping. This approach considers the reactive stream as a (semi)continuous mixture with respect to species type, boiling point, molecular weight, etc. The continuous mixture is governed by a set of concentration density functions which are functionally transformed along the reactor by population balance partial differential equations. The numerical resolution of these equations – via finite element methods, for example – leads to a description of the reactive composition along the reactor. This approach has been addressed for HCC by Basak et al (2004) with promising results. On the other hand, the Continuous Lumping exhibits the obvious onus of being an idealization, which may be aggravated by numerical problems associated with heavy numerical integrations over unbounded domains.

In the present work we consider the HCC of Hydrotreated Heavy Vacuum GasOils (H-HVGO) within an approach that can be viewed as an intermediate instance among all above described methods. Our approach can be briefly described by: (i) a refined

molecular based lumping strategy, able to reproduce the feed characterization and cover HCC products with precision; coupled to (ii) a new molecular based HCC chemical reaction network; and (iii) a two-phase equilibrium reactor model.

We start proposing a discrete compositional model of Hydrotreated Heavy Vacuum GasOil (H-HVGO) for HCC reactors. A set of hydrocarbon representatives (i.e. lumps) is formulated to cover relevant functional molecular structures based on available analytical information of H-HVGO and its expected HCC products. Each molecular representative is identified by a set of parameters defining its concentration and a characteristic side chain length. This model is complemented with a framework of auxiliary rules for generation of descendant structures. Model parameters are estimated through non-linear regression, via adherence of predicted properties onto corresponding experimental characterizing assays. We call this step as Phase I.

The reactive model for HCC of H-HVGO was addressed in Phase II of this work. Following the HCC Literature, kinetic rules were formulated for proposing a suitable HCC reaction network from molecule-based kinetic modelling. For this network, a two-phase equilibrium reactor model was developed for prediction of isothermal HCC. With characterization data of isothermal HCC products, obtained via pilot plant HCC runs, we estimated the primary parameters – fundamental kinetic and adsorption coefficients – of the HCC reaction network.

The remainder of this work is organized as follows. Section 2 introduces the compositional model for H-HVGO, whose parameters were estimated in Section 3. Section 4 approaches the proposed HCC reaction network for H-HVGO. Section 5 addresses the isothermal HCC reactor model. Results of the estimation of the primary HCC parameters are presented in Section 6. Section 7 ends the paper with our conclusions and final comments.

2. Compositional Model for Hydrotreated Heavy Vaccum Gasoil (H-HVGO)

The H-HVGO is characterized by the physical-chemical assays shown in Table 1. In order to allow H-HVGO molecular modeling (and posterior HCC simulation), the proposed set of species must be (directly or indirectly) identifiable from the assays in Table 1 and must cover the spectrum of reactive functional groups relevant to HCC transformations. The constitution of the original HVGO suggests that aromatic molecules with one to five rings are important in this representation. Due to the profound HDT step to prepare the H-HVGO, one may expect that molecules with one to five naphthenic rings mixed with aromatic rings as well phenyl-aromatics resulting from the destruction of heteroatom species, are also important. Finally, paraffins in the diesel range and above, are likely to exist and should not be forgotten.

Having this in mind, 39 representative hydrocarbon species (lumps) were chosen. Firstly a discrete set of 13 primary lumps was formulated: 2 branched paraffins and 11 aromatics (Fig. 2). The remaining 26 species were chosen as partially hydrogenated descendants from the aromatic species. Figure 2 depicts 35 members of

this list of 39 chosen lumps. The representatives not shown are partial hydrogenated descendants of the two phenyl-(poly)aromatics (Fig. 2).

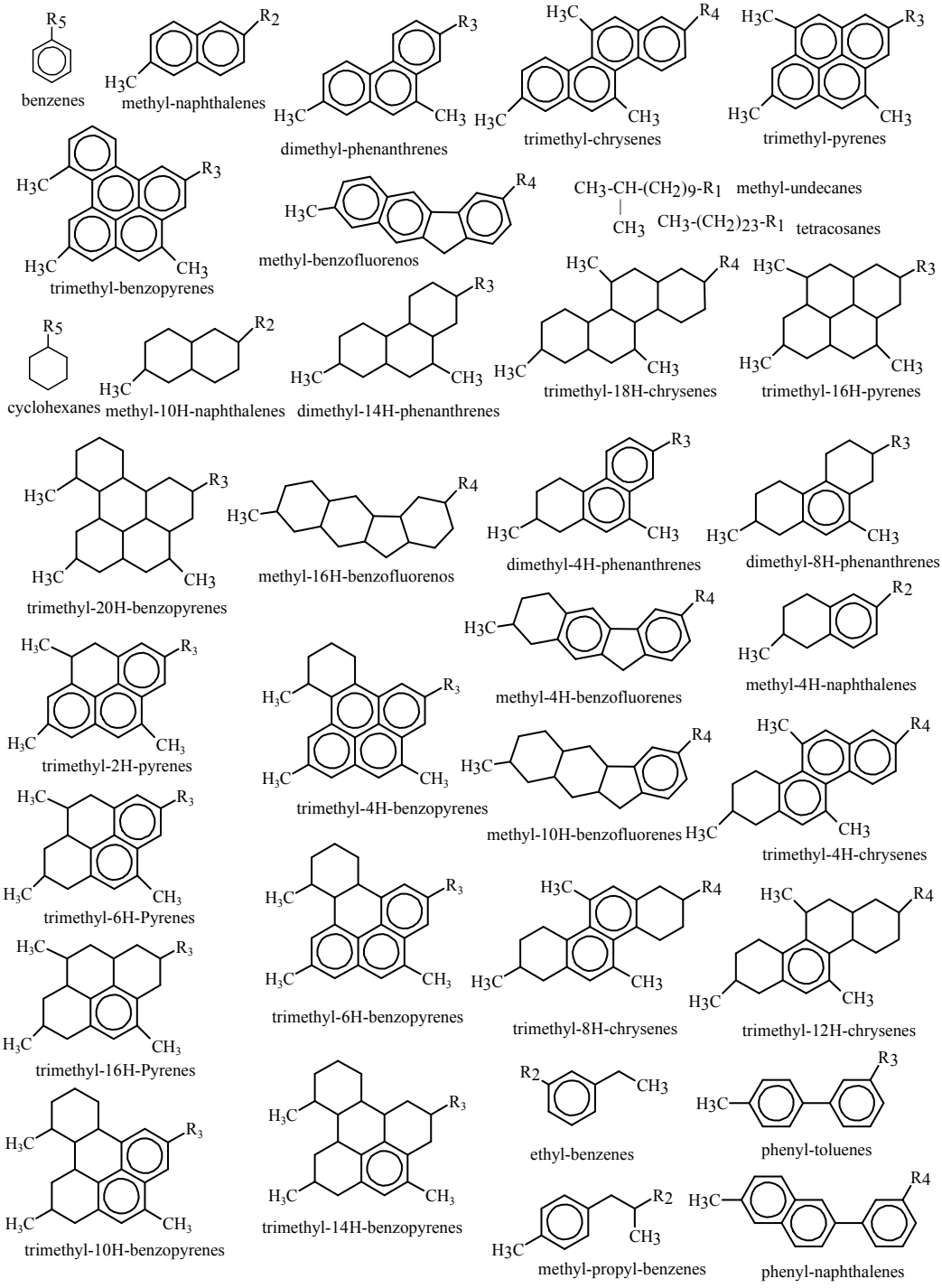

Figure 2: H-HVGO Compositional Model : 35 (of 39) Molecular Representatives

In order to expand the margin of manoeuvre of the compositional model, specially in connection with the matching of distillation ranges, five independent lengths of lateral alkyl chains – *R1, R2, R3, R4, R5* – were assigned to the 13 primary species and inherited by the respective (partial) hydrogenated descendants (see Fig. 2). The Quann-Jaffe rules (Quann-Jaffe, 1996) for defining homologous structures from mono and poly-ring species via attachment of lateral chains, were followed in this concern.

The vector of independent parameters of the H-HVGO compositional model ($\underline{\hat{\theta}}$) has thus, 44 parameters, including all 39 concentrations of lumps – $C_1, C_2, \ldots, C_{39}$ (gmol/100g) – and the 5 numbers of carbons in *R1, R2, R3, R4, R5*. In this model, compounds with 5 rings are descendants by hydrogenation of benzo-pyrenes, whereas molecules with 4 rings are descendants (by hydrogenation) of chrysenes, pyrenes and benzo-fluorenes. Monoaromatics are represented by three benzenic lumps with different lengths of alkyl ramification.

Table 1. Physical-Chemical Assays for Characterization of H-HVGO

Physical-Chemical Properties	Units	No. of Values	Methods
Specific Gravity @ 20/4°C	---	1	ASTM D-4052-96
Kinematic Viscosity @ (20°C,40°C,60°C,100°C)	cSt	4	ASTM D-445-03
Refractive Index @ 20°C	----	1	ASTM D-1747-99
Hydrogen via Low Resolution NMR	%w	1	Petrobras (Gautier-Quignard, 1995)
Simulated Distillation Temperatures (0.5%, 5%, 10%, 30%, 50%, 70%, 90%, 95%, 99.9%)	°C	9	ASTM D-2887-03
Aromatics (mono, bi and tri-aromatics)	mmol/100g	3	IFP
Poly-aromatics Distribution (naphthalenes, phenanthrenes, benzo-fluorenes, chrysenes, pyrenes, benzo-pyrenes	%w	6	Chevron
NMR H1 and C13	%mol	9	Petrobras (Hasan *et al.*, 1983)
Supercritical Fluid Chromatography (SFC)	%w	5	ASTM D-5186-96
Mass Spectrometry (MS)	%v	16	Chevron (Teeter, 1985)
ndM Carbon Distribution (aromatic, naphthenic, paraffinic)	%w	2	ASTM D-3238-95

3. Parameter Estimation of Compositional Model for H-HVGO

The estimation of the *p=44* model parameters ($\underline{\hat{\theta}}$) is done reconciling predictions ($\underline{\hat{Y}}(\underline{\hat{\theta}})$) with the list of H-HVGO characterizing data ($\underline{E}$) (Table 1). To the *57* property values in Table 1 we added an artificial assay referent to a mixture mass of 100g in order to define a basis. Thus the parameter estimation of the compositional model involves *n=58* observed responses, chased by the estimated ones by forcing statistical adherence of $\underline{\hat{Y}}(\underline{\hat{\theta}})$ on $\underline{E}$. The pressure for adhering predictions is adjusted via statistical weighting based on the variance-covariance matrix of $\underline{E}$, written in terms

of a known matrix $\underline{\underline{W}}$ (Eq. (1)). Assays are supposed uncorrelated and normally distributed around correct values, so $\underline{\underline{W}}$ is diagonal. Estimation is performed via Maximum Likelihood leading to a restricted weighted residue minimization (Eq. (2)), solved by a non-linear optimization technique like the Restricted Simplex Method (Barbosa et al., 2003, de Medeiros et al., 2004). Statistics S_R^2 (Eq. (3)) is an estimator for the unknown basic variance σ_E^2 (Eq. (1)). S_R^2 reports a mean quadratic deviation of predictions from observations. Predicted properties ($\underline{\hat{Y}}(\underline{\hat{\theta}})$) are obtained by models (Reid et al., 1987) shown in Table 2. For critical constants, acentric factor, molecular mass and normal boiling point of species i ($T_C(i), P_C(i), \omega(i), MM(i), T_B(i)$) the group contribution method of Joback (Reid et al., 1987) is used. In Table 2 *MD(k,i)* represents the distilled mass of species *i* at temperature T_k.

$$\underline{\underline{COV}}(\underline{E}) = \sigma_E^2 \underline{\underline{W}}^{-1} \tag{1}$$

$$Min\ \ \Psi = (1/2)(\underline{\hat{Y}}(\underline{\hat{\theta}}) - \underline{E})^t \cdot \underline{\underline{W}} \cdot (\underline{\hat{Y}}(\underline{\hat{\theta}}) - \underline{E}) \qquad \{\underline{\theta}_L \le \underline{\hat{\theta}} \le \underline{\theta}_U\} \qquad \{\underline{\hat{\theta}}\} \tag{2}$$

$$S_R^2 = \frac{(\underline{\hat{Y}}(\underline{\hat{\theta}}) - \underline{E})^t \cdot \underline{\underline{W}} \cdot (\underline{\hat{Y}}(\underline{\hat{\theta}}) - \underline{E})}{n - p} \tag{3}$$

Table 2. Methods for Estimation of H-HVGO Properties

Property	Method	Formula	Unity
Total Mass	---	$MT = \sum_i C_i . MM(i)$	g
Total Volume	Rackett and Ideal Solution	$VT(T) = R * \sum_{i=1}^{n_c} \frac{C_i * T_c(i) * ZRA(i)^{\left[1+\left(1-\frac{T}{T_c(i)}\right)^{\frac{2}{7}}\right]}}{P_c(i)}$ $ZRA(i) = 0.29056 - 0.08775 * \omega(i)$	cm^3
Density	Ideal Solution	$\rho = \frac{MT}{VT(T)}$, $T = 293.16\ K$	g/cm^3
Density	Orbey-Sandler	$\rho^{OS}(T) = \frac{MM^{OS}(T_b^{mix})}{\bar{V}^{OS}(T_b^{mix}, T)}$	g/cm^3
Viscosity	Orbey-Sandler	$\mu^{OS}(T) = 0.225 * \left(\mu_R\left(T_b^{mix}, T\right)\right)^{K\left(T_b^{mix}\right)}$	cP
Kinematic Viscosity	Orbey-Sandler	$\nu = \frac{\mu^{OS}(T)}{\rho^{OS}(T)}$	cSt
Mean Boiling Point	Orbey-Sandler	$T_b^{mix} = \left(\sum_i C_i T_B(i)^3 / \sum_i C_i\right)^{1/3}$	K
% Distilled at T_k	True Boiling Point Distillation	$\%D(T_k) = 100. \sum_i MD(k,i) / MT$	%w/w

Estimated parameters for H-HVGO are displayed in Table 3. In addition to the 44 compositional parameters, corresponding to Fig. 2 and manipulated by the optimizer, we pre-fixed manually other 20 concentrations of complementary lumps in order to enhance the adherence to distillation temperatures.

Concentration parameters (C_i) can be expressed as gmol/100g (Table 2) or as g/100g (Table 3), whereas lateral chain sizes *R1, R2, R3, R4, R5* are dimensionless. Table 4 displays the comparison of experimental versus predicted values for some properties. The achieved S_R^2 value was 104.2.

Table 3 : Estimated Parameters # for the Compositional Model of H-HVGO

Lumps	C_i (g/100g)	R_X	Lumps	C_i (g/100g)	R_X
cyclohexanes [30]	0.611	5	trimethyl-benzopyrenes [121]	0.009	3
ethyl-cyclohexanes [2]	11.30	2	trimethyl-4H-benzopyrenes [122]	0.207	3
phenyl-toluenos [3]	0.850	3	trimethyl-6H-benzopyrenes [123]	0.030	3
phenyl-naphthalenes [11]	0.038	4	trimethyl-10H-benzopyrenes [124]	0.597	3
phenyl-4H-naphthalenes [12]	0.477	4	trimethyl-14H-benzopyrenes [125]	0.718	3
phenyl-10H-naphthalenes [15]	0.089	4	trimethyl-20H-benzopyrenes [126]	0.855	3
cyclohexyl-10H-naphthalenes [16]	0.516	4	methyl-undecanes [136]	4.294	1
methyl-naphthalenes [32]	0.254	2	tetracosanes [142]	0.695	1
methyl-4H-naphthalenes [33]	1.910	2	methylbutyl-cy [35]	0.345	2
methyl-10H-naphthalenes [34]	15.74	2	isobutyl-methyl-methylbutyl-cy [46]	0.113	3
dimethyl-phenantrenes [41]	0.104	3	methyl-10H-naph [57]	4.128	3
dimethyl-4H-phenantrenes [42]	0.504	3	isobutyl-dimethyl-10H-naph [56]	0.424	3
dimethyl-8H-phenantrenes [43]	2.524	3	methyl-10H-naph [83]	1.018	4
dimethyl-14H-phenantrenes [44]	14.42	3	isobutyl-dimethyl-methylbutyl-10H-naph [80]	2.045	4
trimethyl-chrysenes [63]	0.179	4	ethylmethylhexyl-dimethyl-10H-naph [81]	0.737	4
trimethyl-4H-chrysenes [64]	0.101	4	methyl-methylpropyl-hexyl-10H-naph [82]	0.001	4
trimethyl-8H-chrysenes [65]	2.926	4	methyl-methylbutyl-10H-naph [45]	0.117	3
trimethyl-12H-chrysenes [66]	0.102	4	isobutyl-trimethyl-14H-phen [73]	1.214	4
trimethyl-18H-chrysenes [67]	6.992	4	dimethyl-methylbutyl-14H-phen [74]	7.021	4
benzenes [29]	0.211	5	ethylpropyl-dimethyl-16H-pyr [133]	0.318	3
ethyl-benzenes [1]	2.424	2	dimethyl-octadecanes [144]	0.028	1
isobutyl-methyl-benzenes [27]	0.792	2	dimethyl-dodecanes [148]	0.010	1
methyl-benzofluorenes [106]	0.035	4	trimethyl-octanes [36]	0.300	2
methyl-4H-benzofluorenes [108]	0.066	4	ethyl-trimethyl-undecanes [47]	0.092	3
methyl-10H-benzofluorenes [109]	0.135	4	benzenes [38]	0.013	2
methyl-16H-benzofluorenes [110]	4.233	4	ethylmethylhexyl-dimethyl-4H-naph [78]	0.182	4
trimethyl-pyrenes [111]	0.096	3	isobutyl-dimethyl-methylbutyl-4H-naph [86]	0.135	4
trimethyl-2H-pyrenes [112]	0.377	3	methyl-naph [58]	0.691	3
trimethyl-6H-pyrenes [115]	0.091	3	Where $R_1 = 2.33$ / $R_2 = 15.16$		
trimethyl-10H-pyrenes [116]	2.830	3	$R_3 = 0.02$ / $R_4 = 12.40$		
trimethyl-16H-pyrenes [117]	2.734	3	$R_5 = 1.1$		

: 64 parameters are shown, the truly estimated 39 C_i's + 5 R_i's added to 20 pre-fixed C_i's of complementary species ([.] : lump index in the full HCC model, i.e. including HCC products)

$R_X = R_1, R_2, R_3, R_4, R_5$, cy:cyclohexanes, naph:naphthalenes, phen:phenantrenes, pyr = pyrenes

Table 4 : Experimental versus Predicted Property Values after Parameter Estimation for the Compositional Model of H-HVGO

Property	Units	Experimental	Estimated	Deviation (%)
Density 20°C/4°C		0.8879	0.8829	-0.56
Kin. Viscosity 60°C / 100 °C	cSt	11.43 / 4.253	9.837 / 5.067	-13.9 / 19.1
Sim. Dist. Temperatures D-2887				
0.5% / 10 %	°C	107 / 259	106 / 256	-0.93 / -1.16
30% / 50 %	°C	358 / 410	350 / 417	-2.23 / 1.71
70% / 90 %	°C	449 / 497	453 / 508	0.89 / 2.21
95% / 99.9 %	°C	516 / 558	511 / 550	-0.97 / -1.43
Aromatics Chevron				
Naphthalenes / Phenantrenes	%w	0.89 / 0.10	0.98 / 0.104	10.1 / 4.0
Benzofluorenes	%w	0.036	0.0357	-0.83
Chrysenes / Pyrenes	%w	0.153 / 0.097	0.179 / 0.096	17.0 / -1.0
Benzopyrenes + Perylenes	%w	0.0083	0.0085	2.4
NMR				
Chain Size		15.0	12.1	-19.3
C Aromatic / C Saturated	%mol	6.1 / 93.9	7.9 / 92.1	29.5 / -1.92
H Aromatic / H Saturated	%mol	2.7 / 97.3	1.8 / 98.2	-33.3 / 0.92
SFC				
Saturated	%w	79.8	80.31	0.64
Mono / Diaromatics	%w	12.1 / 6.9	12.06 / 6.45	-0.33 / -6.5
Tri / Polyaromatics	%w	0.7 / 0.5	0.69 / 0.49	-1.43 / -2.0
Mass Spectrometry				
Paraffins	%v	6.5	6.25	-3.8
Mono / Dinaphthenics	%v	28.6 / 26.6	12.7 / 25.6	-55.6 / -3.8
Tri / Tetra-naphthenics	%v	17.8 / 7.5	22.6 / 13.8	27.0 / 84.0
Penta-naphthenics	%v	0.0	0.82	---

With the jacobian matrix of predictions to parameters ($\underline{\underline{J}}^T = \left[\underline{\nabla}_\theta \underline{\hat{Y}}^T\right]$), several statistic entities can be accessed. The variance-covariance matrices for estimated parameters and model responses are respectively estimated by Eqs. (4) below:

$$\underline{\underline{C\hat{O}V}}(\underline{\hat{\theta}}) = S_R^2\left[\underline{\underline{J}}^T \underline{\underline{W}}\,\underline{\underline{J}}\right]^{-1} \tag{4a}$$

$$\underline{\underline{C\hat{O}V}}(\underline{\hat{Y}}) = S_R^2\,\underline{\underline{J}}\left[\underline{\underline{J}}^T \underline{\underline{W}}\,\underline{\underline{J}}\right]^{-1}\underline{\underline{J}}^T \tag{4b}$$

Standard deviations of estimated parameters and responses are then obtained with:

$$\hat{\sigma}_{\hat{\theta}i} = \sqrt{\left[\underline{\underline{C\hat{O}V}}(\underline{\hat{\theta}})\right]_{ii}} \qquad (i = 1...p) \tag{5a}$$

$$\hat{\sigma}_{\hat{Y}i} = \sqrt{\left[\underline{\underline{C\hat{O}V}}(\underline{\hat{Y}})\right]_{ii}} \qquad (i = 1...n) \tag{5b}$$

The confidence region for true parameters ($\underline{\theta}$) at level $1-\alpha$ ($\alpha = 0.01$) is given by:

$$(\underline{\theta} - \underline{\hat{\theta}})^T \left(\underline{\underline{J}}^T \underline{\underline{W}} \underline{\underline{J}}\right)(\underline{\theta} - \underline{\hat{\theta}}) \leq pS_R^2 \phi_{1-\alpha} \tag{6}$$

Where $\phi_{1-\alpha}$ is the Fisher abscissa for probability $1-\alpha$ and degrees of freedom ($p, n-p$). Finally, confidence intervals for true parameters ($\underline{\theta}$) and true responses ($\underline{Y}$) at level $1-\alpha$ ($\alpha = 0.01$), follow by Eq. (7) below:

$$\hat{\theta}_i - t_{1-\alpha/2}\sqrt{\left[\underline{\underline{C\hat{O}V}}(\underline{\hat{\theta}})\right]_{ii}} < \theta_i < \hat{\theta}_i + t_{1-\alpha/2}\sqrt{\left[\underline{\underline{C\hat{O}V}}(\underline{\hat{\theta}})\right]_{ii}} \qquad (i = 1...p) \tag{7a}$$

$$\hat{Y}_i - t_{1-\alpha/2}\sqrt{\left[\underline{\underline{C\hat{O}V}}(\underline{\hat{Y}})\right]_{ii}} < Y_i < \hat{Y}_i + t_{1-\alpha/2}\sqrt{\left[\underline{\underline{C\hat{O}V}}(\underline{\hat{Y}})\right]_{ii}} \qquad (i = 1...n) \tag{7b}$$

Some of these entities are depicted in Figs 3 for the determination of compositional model of H-HVGO. Fig. 3A is a logarithmic plot of predicted versus observed responses. The diagonal alignment is evident, albeit deviations are apparent for some responses. Fig. 3B displays the projection of the 99% confidence region of correct parameters on the plane $\%C_{METHYL\text{-}UNDECANES}$ versus $\%C_{TETRACOSANES}$. Methyl-Undecanes and Tetracosanes are the only paraffin lumps manipulated in the parameter estimation. Fig. 3B reveals that the tuning for Methyl-Undecanes (with a lateral alkyl chain with 2.33 carbons) was better achieved. Nevertheless, the higher (relative) uncertainty for Tetracosanes is a consequence of the small estimated concentration for this lump. Fig. 3C displays the projection of the 99% confidence region of correct parameters on the plane $\%C_{4H\text{-}DIMETHYL\text{-}PHENANTRENES}$ versus $\%C_{14H\text{-}DIMETHYL\text{-}PHENANTRENES}$. These lumps refer both to species created by the HDT of HVGO. The concentration of 14H-Dimethyl-Phenantrenes seems to be estimated with moderate uncertainty, whereas there is (relatively) higher uncertainty for 4H-Dimethyl-Phenantrenes, again a consequence of a small estimated value. The characteristic oblong form of this projection suggests correlation between these two parameters. Fig. 3D displays estimates for standard deviations of predicted responses. In general, with the exception of a few estimates with huge uncertainties (e.g. the first high peak is the standard deviation of *mmol* of Monoaromatics per 100g by the IFP Method, which is not considered an accurate assay) the standard deviations of estimated responses fall below 20% of the experimental value, which is a reasonable result.

4. Addressing a Chemical Reaction Network for the Hydrocracking of H-HVGO

A chemical reaction network for HCC of H-HVGO is proposed via a molecule-based modelling in the light of the H-HVGO compositional model. Due to space concerns, the network is condensed as in Fig. 4. The HCC reaction network is a set $\mathfrak{R}$ with 235 *elementary direct* chemical reactions. By an *elementary direct* reaction we mean a single, oriented, step of chemical transition. Thus, reversible chemical reactions in broad sense, are described by the allocation of two opposed *elementary direct* reactions of $\mathfrak{R}$. In this work the terms "reaction" or "chemical reaction" is always understood as an *elementary direct* chemical reaction of set $\mathfrak{R}$.

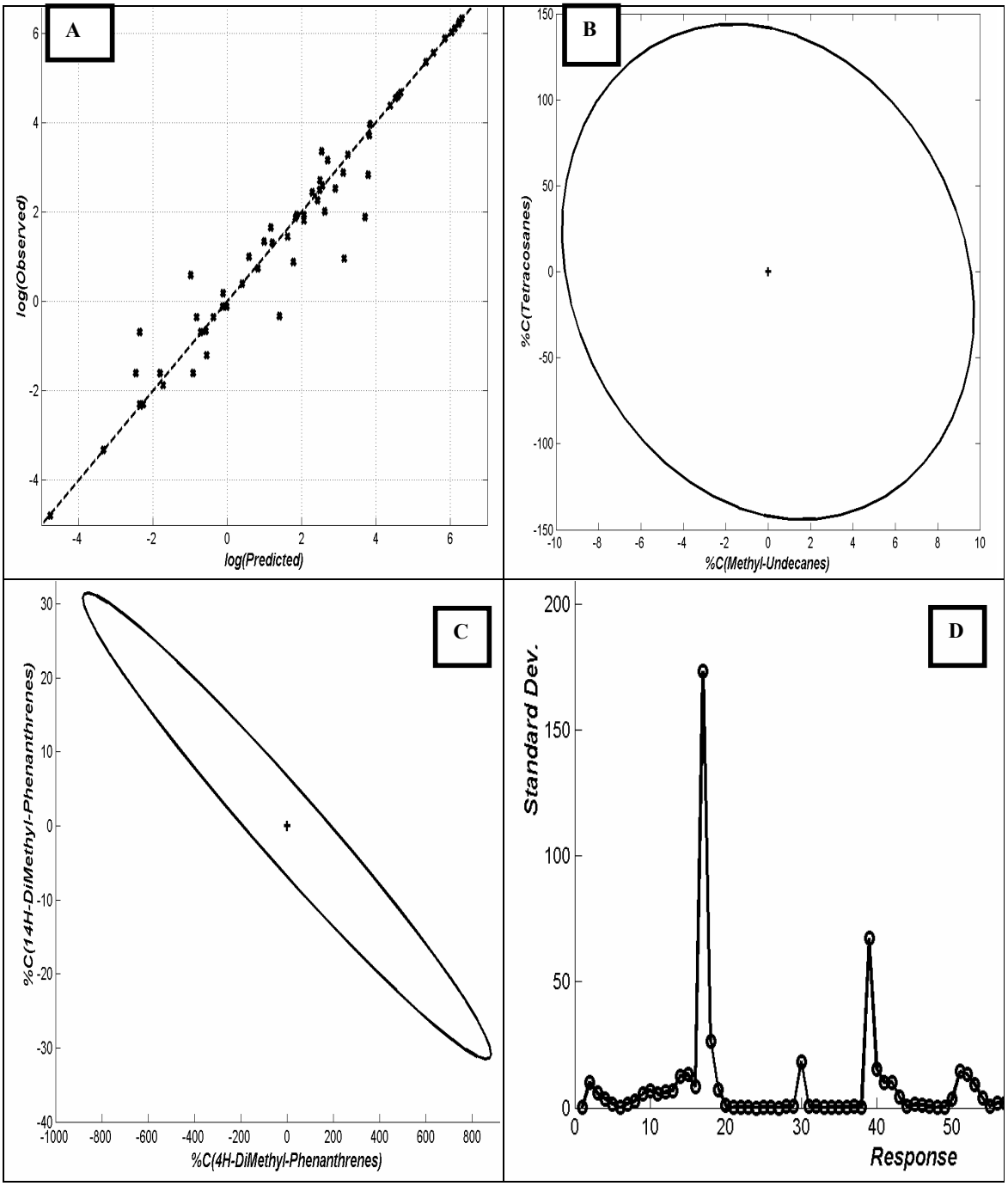

Figure 3: Results of Parameter Estimation for Compositional Model of H-HVGO
[A] log(Observed) vs log(Predicted);
[B] 99%Confidence $C_{METHYL\text{-}UNDECANES}$ vs $C_{TETRACOSANES}$;
[C] 99% Confidence $C_{4H\text{-}DIMETHYL\text{-}PHENANTRENES}$ vs $C_{14H\text{-}DIMETHYL\text{-}PHENANTRENES}$;
[D] Standard Deviations of Estimated Responses

H_2 participates in all reactions of $\mathfrak{R}$. In the majority of reactions H_2 acts as a reactant (i.e. hydrogenation reactions), but there is a minority of reactions that release H_2 (i.e. dehydrogenation reactions of poly-ring naphthenics with at least one aromatic ring, in equilibrium with the corresponding hydrogenation reactions).

All participants species in $\mathfrak{R}$ belong to one of the following three classes J, N or V. Class J contains species that are representatives of lumps and have a lateral alkyl chain belonging to the set $\{R_1,R_2,R_3,R_4,R_5\}$, inherited from the Compositional Model of H-HVGO. Species of Class J have complex structures so their physical constants are estimated by Joback Method. Class N contains species that are representatives of lumps *but do not have* a lateral alkyl chain from the set $\{R_1,R_2,R_3,R_4,R_5\}$ because it was dealkylated by HCC. Species of Class N are also complex enough to have their physical constants estimated by Joback Method. Finally, species of Class V are small (*volatile*) molecules with simple structures whose physical constants are well known and do not need group contribution methods. Species of Class V are H_2, CH_4, C_2H_6, C_3H_8, C_4H_{10}, iC_4H_{10}, C_5H_{12}, iC_5H_{12}, iC_6H_{14}, benzene, toluene, methyl-cyclohexane, iC_7H_{16}, cyclohexane, $C_5H_{11}C_2H_5$, iC_8H_{18}.

The network $\mathfrak{R}$ of reactions involves *nc=158* species and *nr=235* reactions. The *nc=158* species are distributed according to *nj=117* in Class J, *nn=25* in Class N, and *nv=16* in Class V. The 59 species in the Compositional Model of H-HVGO are all of Class J. It must be noted that we have a lump called *benzenes* in Class J and, simultaneously, the species benzene in Class V.

HCC is a complex process, operating on a *per se* complex feed, at severe and dangerous conditions of reactant, temperature, pressure and spatial time. In consequence, it is, by no means, an easy task to acquire useful HCC data from experiments with real feeds. Thus, the HCC network $\mathfrak{R}$ was formulated keeping in mind that a gigantic, exhaustive, reactive representation – i.e. covering a large set of possible chemical transformations and product species in the HCC of H-HVGO – has a material risk of being valueless due to lack of reliable, organized and public data sufficient to define $\mathfrak{R}$ numerically. Consequently, $\mathfrak{R}$ was formulated adopting the following set of simplifying principles and short-cut rules, which are based on reasonable arguments and on the Literature of hydrogenation of Hydrocarbons:

[1] Hydrodesulphurization/Hydrodenitrogenation and olefin saturation occur only during the first stage of hydrotreating, they are not present in HCC.
[2] Saturation of aromatics, dealkylation of side chains from naphthenics/aromatics, and cracking of naphthenics/paraffins are the most important transformations in HCC (H.P.C., 2004).
[3] Cyclization of paraffins (Russell and Klein, 1994), condensation, methyl transfer and other secondary reactions are not supposed to occur in considerable extension.
[4] Isomerization was not considered as an isolated transformation in this model. It was embedded as part of more extent transformations like the ones resulting in the opening of naphthenic rings with 6 carbon atoms (Qader,1973; Russel and Klein,1994; Korre et al.,1995; Hou et al., 1999).
[5] Aromatic ring saturation proceeds in a ring-by-ring manner. Isolated aromatic

rings, peripheral rings in poly-condensed species and internal rings undergo saturation, respectively with 6, 4 and 2 H atoms. Peripheral rings are saturated first (Korre et al, 1995).

[6] Rupture of naphthenic ring, conjugated to an aromatic ring, occurs at the alpha aromatic position, implying that the intermediary carbenium ion will be always secondary or tertiary (Hou et al., 1999).

[7] Aromatic rings are not cracked; they must be saturated first. Only naphthenic rings can be cracked in the fashion cited above. The reactivity of aromatic rings under saturation increases according to the order: mono, di, tri, tetra, penta-aromatics, i.e. a penta-aromatic molecule saturates one ring faster than a monoaromatic one.

[8]Benzopyrenes are hydrogenated/hydrocracked to pyrenes, which are then hydrogenated/hydrocracked to phenanthrenes, according to the sequential mechanism proposed by Qader (1973).

[9] The reverse reaction of aromatics saturation, i.e. dehydrogenation of naphthenics, is defined only for species with at least 2 rings being one of them an aromatic ring (Korre et al.1995); thus a monoaromatic can not be formed from a mononafthenic.

[10]Naphthenic/aromatic dealkylation occurs for side chains with 3 or more paraffinic carbons, with complete liberation of the chain (Hou et al., 1999).

[11]In order to avoid an huge increase of $\Re$, certain reaction products can be substituted by functionally similar, isomer species, already defined in $\Re$, if the Joback Method is not capable to distinguish them.

[12]Paraffins can be cracked if they have 8 or more carbon atoms. Exhaustive alternatives of paraffin cracking are not provided by $\Re$; only a representative set of paraffin (with 8 or more carbon atoms) cracking reactions were defined.

[13]CH_4 and C_2H_6 can only be produced by reactions of thermal cracking of paraffins with 8 or more carbon atoms.

[14]As done in the naphthenics case, the isomerization of paraffins is embedded in the cracking of paraffins. Thus the proposed hydrocracking of paraffins favours increases in the degree of ramification of products, being assumed that these products have at most two methylic ramifications.

[15]Paraffin isomerization occurs via protonated cyclopropane intermediate (PCP), Thus the new ramification is always a methyl. Ethyl ramification via protonated cyclobutane intermediate (PCB), is neglected (Svoboda et al., 1995).

[16]The network $\Re$ allows progressive conversion of all initial naphthenic and aromatic lumps into paraffinic lumps; i.e. $\Re$ can, in principle (i.e. if enough reaction time is allowed) promote the entire hydro-conversion of aromatics and naphthenics into paraffins. In other words, there is no dead-end in $\Re$ which could permit the preservation of naphthenics and aromatics at the outlet of a sufficiently large HCC reactor.

Figure 4 depicts a condensed view of the chemical reaction network ($\Re$) for HCC of H-HVGO. Two important sectors of $\Re$ are detailed in Fig. 5, namely, the main routes of hydro-conversion of naphthalenes and benzo-pyrenes. Fig. 6 offers a view of the non-zero positions inside the stoichiometric matrix $\underline{\underline{H}}$ of $\Re$ (size *nc x nr*). Columns of $\underline{\underline{H}}$ refer to reactions, while rows refers to species (or lumps). Row 118, with no zero elements, corresponds to H_2. The number of non-zero positions is 784.

A network of chemical reactions for modeling hydrocracking reactors

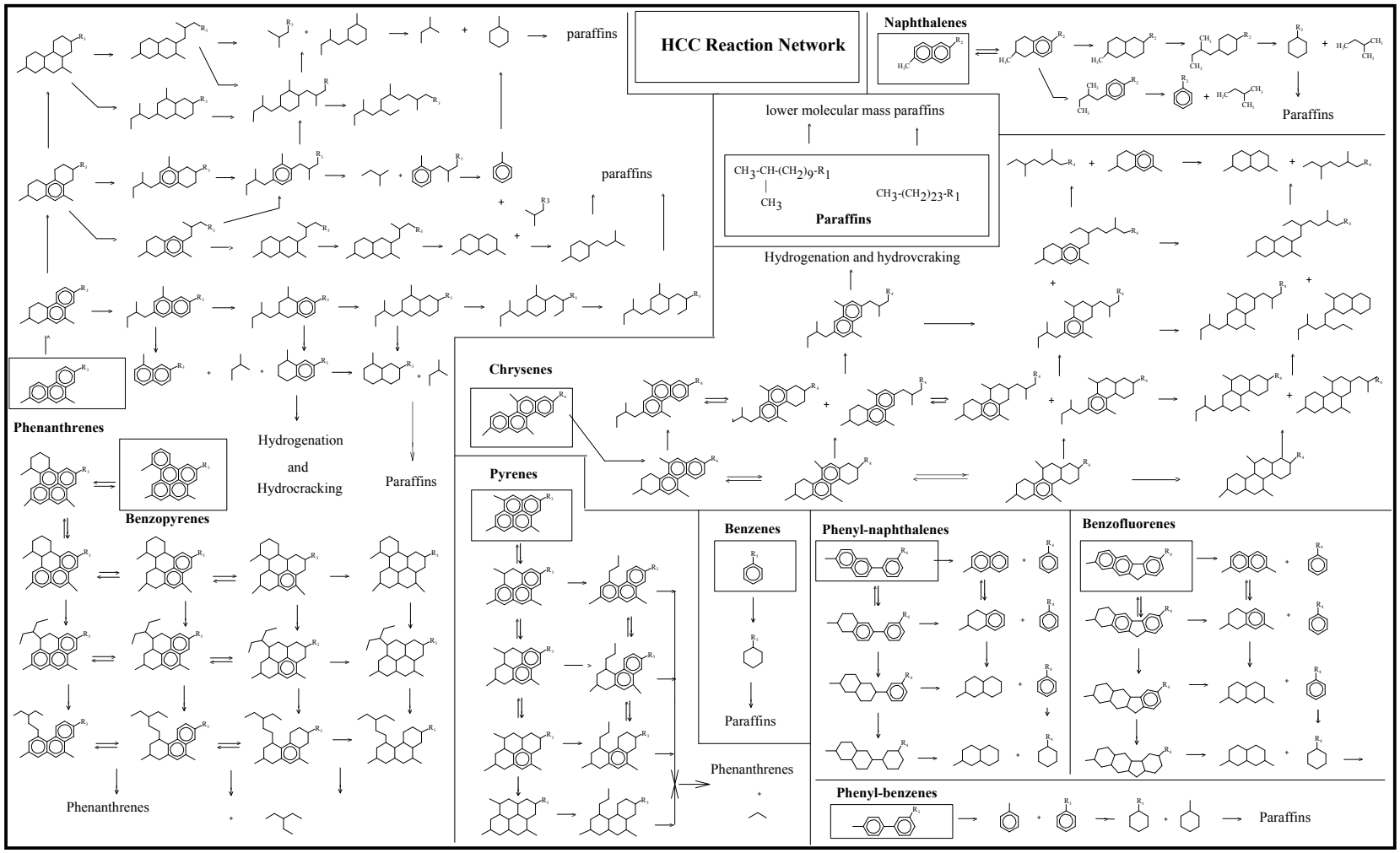

Figure 4: Chemical Reaction Network for HCC of Hydrotreated Heavy GasOil

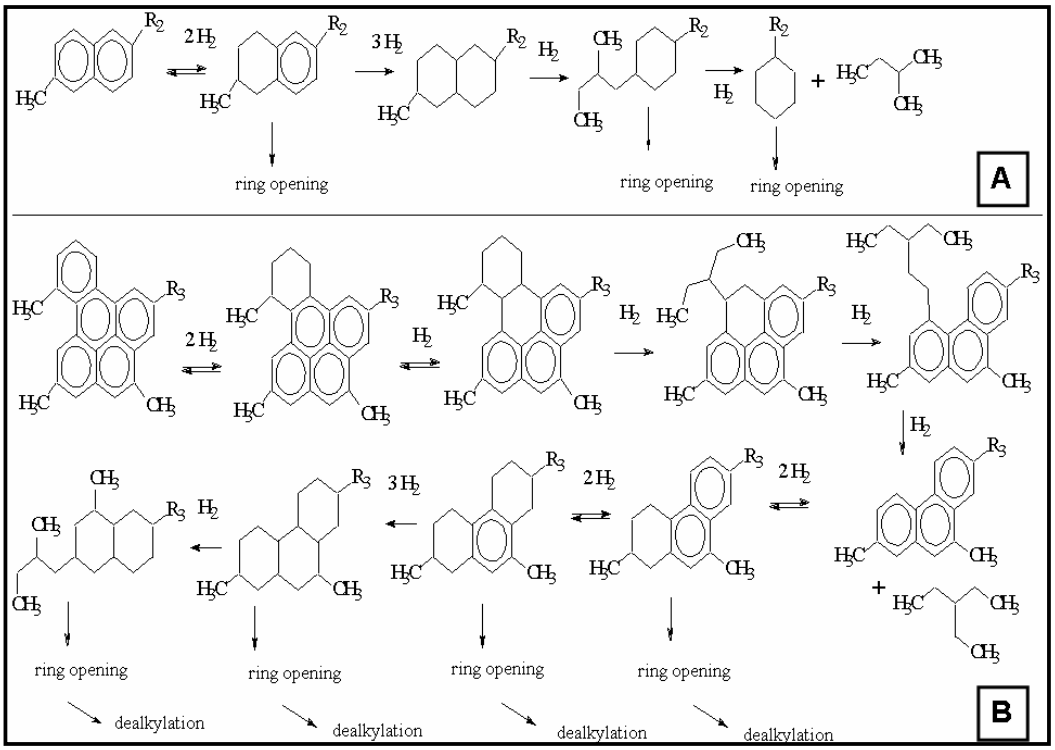

Figure 5: Sectors of the HCC Network of H-HVGO
[A] : Main Route for Hydro-Conversion of Naphthalenes
[B] : Main Route for Hydro-Conversion of Benzo-Pyrenes

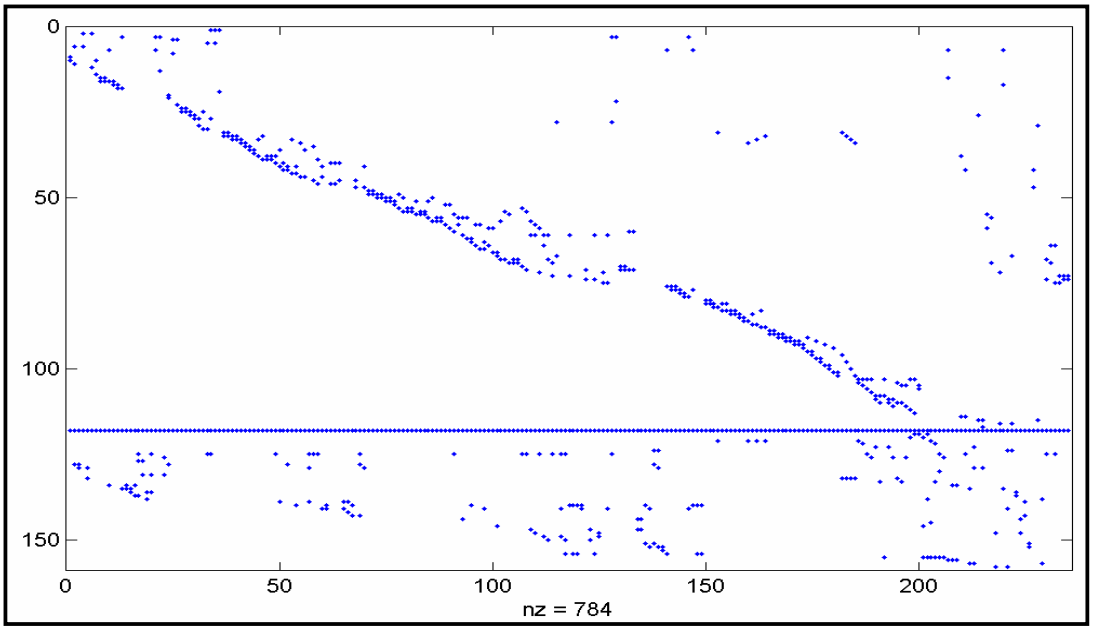

Figure 6: View of the Non-Zero Pattern of the Stoichiometric Matrix ($\underline{\underline{H}}$) of $\Re$

The operational definition of the HCC network demands the assignment of kinetic rules and mechanisms to all *nr=235* chemical reactions of $\Re$. Since HCC involves high temperatures (above 300°C), high pressures (above 100bar), high hydrogen/hydrocarbon ratios (above 500NL/kg) and high turbulent flow in trickle-bed reactors, it is a common practice (Martens and Marin, 2001) to neglect radial gradients of composition and mass transfer resistances. That is, both bulk liquid and gas phases, as well the adsorbed phase on the catalyst, are supposed very near to thermodynamic equilibrium along the reactor axis. Additionally, composition profiles are relevant only along the axial direction through the bed.

In this context, each reaction has its rate defined uniquely by its own kinetic model and mechanism. The reaction kinetic model, by its turn, would be dependent only on the distribution of species fugacities along the bed, coupled to an adsorption model (e.g. Langmuir adsorption) to take the interaction with the catalyst into account. On the other hand, if one realize that each species lump should have one Langmuir adsorption coefficient (temperature dependent) and each reaction should have one rate coefficient (temperature dependent), the number of parameters in the HCC model would be impracticably high to be estimated. In face of this, a reduction on the number of independent parameters was implemented.

Firstly the number of kinetic rules was reduced from 235 to 75 by assigning the same kinetic rule to similar reactions; that is, representing $K_{L(k)}$ the kinetic coefficient assigned to reaction *k*, it can be shared by another reaction *m*, such that $K_{L(k)} = K_{L(m)}$, where $L(k)$ is the kinetic index used by reaction *k*. The number of kinetic rules is represented by *nk* (*nk=75*). Secondly, the *nk=75* kinetics were arranged into two groups: (i) a group of 17 primary kinetics; and (ii) a group of 58 secondary kinetics. The primary kinetics are assumed independent. The secondary kinetics are calculated from the primary ones through proportionality factors suggested in the Literature (Qader, 1973; Russel and Klein, 1994; Korre et al., 1995, 1997; HPC, 2000; Hou et al., 1999; Martens and Marin, 2001, da Silva, 2007). Table 5 presents the primary kinetics for the HCC network. The secondary kinetic coefficients are calculated from the primary ones by proportionality factors as presented in da Silva (2007).

A similar procedure separated the *nc=158* Langmuir coefficient into two groups:
(i) a group of 2 primary (independent) Langmuir coefficients: K_{H2}^{ADS}, K_{C6H6}^{ADS}.
(ii) a group with the remaining 156 Langmuir coefficients.

Due to its intrinsic importance, H_2 will keep its own Langmuir coefficient in the formalism. All other hydrocarbon will have the respective Langmuir coefficient posed in terms of the coefficient of Benzene; i.e. all secondary Langmuir coefficients for the 156 remaining hydrocarbons are assumed proportional to the reference Langmuir coefficient of Benzene (C_6H_6). The proportionality factors are estimated with the correlations of Korre et al. (1997).

The total number of independent kinetc+adsorption parameters (all as functions of temperature) of the network of HCC reactions is, therefore, *np=17+2=19.*

Table 5 – Primary Kinetic Rules for HCC Reaction Network

No.	Kinetic	Description
1	1B +H	Monoaromatics Hydrogenation (+H)
2	2B +H	Diaromatics Hydrogenation (+H)
3	2B –H	Diaromatics Hydrogenation - Reverse Reaction (-H)
4	3B +H	Triaromatics Hydrogenation (+H)
5	3B -H	Triaromatics Hydrogenation - Reverse Reaction (-H)
6	BB -C	Hydrocracking of phenyl-aromatics
7	B –R	Dealkylation of monoaromatics
8	F -R	Dealkylation of mononaphthenics
9	1F -C	Hydrocracking of mononaphthenics
14	2F -C	Hydrocracking of dinaphthenics
15	3F -C	Hydrocracking of trinaphthenics
37	4F -C	Hydrocracking of tetra-naphthenics
65	5F -C	Hydrocracking of penta-naphthenics
10	R12 -3C	Hydrocracking of paraffins with release of C_3H_8
11	R24 -4C	Hydrocracking of paraffins with release of C_4H_{10}
12	R24 -C	Hydrocracking of paraffins with release of CH_4
13	R24 -2C	Hydrocracking of paraffins with release of C_2H_6

5. HCC Reactor Model

As written before, the heterogeneous HCC reactor is supposed in stationary regime with only one independent spatial coordinate, namely the axial position z (m). The spatial time t (kg^{CAT}/(kg/h)) can be expressed in terms of z, the catalyst density ρ^{CAT} (kg/m^3), the reactor area section A (m^2) and the flow rate of feed F_0 (kg/s) by Eq. (8) below.

$$t = z * A * \rho^{CAT} / F_0 \qquad (8)$$

After defining the independent variable (t), the dependent variables are defined as the component fluxes (for lumps J and N; and V components) given as molar rates (gmol/s) along the reactor ($\underline{N}(t)$, $\underline{N}_0=\underline{N}(t=0)$).

Since the development of this HCC model is supported by Pilot Plant HCC runs, which are nearly isothermal continuous runs, the proposed reactor model must refer to isothermal steady flow regime. The adaptation of this model to the industrial adiabatic reactor is reasonably straightforward; despite the lot of attention that have to be paid, in this last case, to: (i) accuracy of prediction of thermal effects and/or the enthalpy flux along the bed; (ii) quenching concerns; (iii) temperature profile and its influence on the profiles of reaction rates, vaporized fraction and vapor/liquid compositions along the bed. The industrial reactor will be addressed in a future work.

For developing the reactor model the following main assumptions are made:

[1] Two-phase isothermal (or under a known temperature profile) steady cocurrent flow of gas and liquid permanently under multicomponent Vapor-Liquid Equilibrium (VLE) is assumed; so that component fugacities are well defined and uniform along the phases at the same reactor location.

[2] A steady, basically linear and known, pressure profile is assumed.

[3] Equilibrium between bulk phases and the catalyst adsorbed phase along the reactor via Langmuir adsorption equilibrium.

[4] Reaction rates are supposed to affect both phases; i.e. there is no reason to confine reactions just in one phase. Thus we model reaction rates in terms of fugacities which are uniformized properties across the phases at the same reactor location.

[5] Fugacity representation for calculating reaction rates – in place of the usual partial pressures or concentrations – is a valid option because, in view of the high pressures, temperatures and hydrogen/hydrocarbon ratios involved (100-200bar, 300-400 ^{o}C, 500-2000 NL/kg), gas and liquid phases are far from the usual idealized condition of ideal gas and dilute incompressible liquid, respectively. As a matter of fact, the gas phase has about 2% mol of heavy hydrocarbons and 98% mol of H_2, which means about 50% mass of hydrocarbon; at the same time the liquid has 30% mol of dissolved H_2. Thus both phases are simultaneously dense and compressible, entailing that it is mandatory to consider non ideality effects in both phases of HCC models.

[6] Component fugacities are calculated along reactor spatial integration via resolution of VLE with *Flash(T,P,N)* algorithms for each point where reaction rates are required. Conventional Cubic Equations of State (Peng-Robinson or Soave-Redlich-Kwong) are used in both phases for flash calculations and thermodynamic property estimation.

[7] Critical and physical constants of species (lumps) are estimated via Joback Method if necessary.

[8] Each reaction rate is calculated with one of four possible reaction mechanisms, which were chosen as the most relevant alternatives (see below).

With these assumptions, the vector $\underline{R}$ of reactions rates (expressed in gmol/s.kg^{CAT}, with size *nr x 1*) is written in terms of temperature T (K) and the vector of component fugacities $\underline{f}$ (bar) according to Eq. (9) below:

$$\underline{R}(T,\underline{f}) = \underline{\Psi}(T,\underline{f}) \bullet \left\{ \underline{\underline{Diag}}(\underline{\underline{D}}\,\underline{K}(T)) \left\{ \underline{\underline{S}}^{AD} \left(\underline{K}^{AD}(T) \bullet \underline{f} \right) + \underline{\underline{S}}^{NAD}\,\underline{f} \right\} \right\} \qquad (9)$$

In this formula $\bullet$ expresses multiplication between correspondent elements of two vectors of same size; $\underline{\underline{Diag}}$ creates a diagonal matrix from a vector; $\underline{K}(T)$ is the *nk x 1* vector of *nk=75* kinetic coefficients; $\underline{K}^{AD}(T)$ is the *nc x 1* vector of Langmuir component coefficients; $\underline{\Psi}(T,\underline{f})$ is a *nr x 1* vector referring to caracteristic rate terms invoked by reaction mechanisms as defined below; and $\underline{\underline{D}}$, $\underline{\underline{S}}^{AD}$, $\underline{\underline{S}}^{NAD}$ are operator matrices (sizes given, respectively, by *nr x nk, nr x nc, nr x nc*) such that:

$D_{km} = 1 \Rightarrow$ reaction *k* uses kinetic *m*, otherwise $D_{km} = 0$

$S_{kj}^{AD} = 1 \Rightarrow$ rate of reaction *k* is defined by adsorbed species *j* , otherwise $S_{kj}^{AD} = 0$

$S_{kj}^{NAD} = 1 \Rightarrow$ rate *k* is defined by species *j* in fluid phase, otherwise $S_{kj}^{NAD} = 0$

Mechanisms for HCC Reaction Rates

The rate of reaction *k,* R_k (gmol/s.kg^{CAT}), using kinetic coefficient $K_{L(k)}$, is defined by a main hydrocarbon reactant *i* according to one of four possible basic mechanisms expressed in the Langmuir-Hinshelwood format (da Silva, 2007):

- Mechanism 1 : *[H_2(Ads)+HC(Fluid)]*
  This mechanism proposes rate controlled by slow reaction between adsorbed H_2 (no dissociated) and hydrocarbon *i* from the bulk phases (both order 1):

$$R_k = K_{L(k)} f_i \left(\frac{K_{H2}^{ADS} f_{H2}}{1 + \sum_j^{nc} K_j^{ADS} f_j} \right) \tag{10a}$$

- Mechanism 2 : *[HC(Ads)-H]*
  In dehydrogenation reactions (i.e. for poly-naphthenics with at least one aromatic ring), the mechanism involves the equilibrium adsorption of the hydrocarbon on the catalyst followed by slow (order 1) liberation of hydrogen:

$$R_k = K_{L(k)} \left(\frac{K_i^{ADS} f_i}{1 + \sum_j^{nc} K_j^{ADS} f_j} \right) \tag{10b}$$

- Mechanism 3 : *[H_2(Fluid)+HC(Fluid)]*
  For thermal paraffin cracking reactions (producing CH_4, C_2H_6) the controlling reaction occurs in the fluid phase with order 1 for both reactants:

$$R_k = K_{L(k)} f_i f_{H2} \tag{10c}$$

- Mechanism 4 : *[H_2(Fluid)+HC(Fluid)]*
  This mechanism follows an argument (Froment, 1987) that pressure inhibition (in fact, hydrogen inhibition) affects the hydrocracking of paraffins adsorbed on metallic sites. Inhibition is associated with the precocious saturation of an olefinic precursor of cracking formed on the catalyst. The rate formula is:

$$R_k = K_{L(k)} \left(\frac{K_i^{ADS} f_i}{\Omega(f_{H2}) \left(1 + \sum_j^{nc} K_j^{ADS} f_j \right)} \right) \quad , \ \Omega(f_{H2}) = f_{H2} / 150 \tag{10d}$$

With Eqs. (10), the definition of rate terms $\underline{\Psi}(T,\underline{f})$ in Eq. (9) are given below:

$$\Psi_k(T,\underline{f}) = \begin{cases} = \dfrac{K_{H2}^{AD} f_{H2}}{1+\sum_j^{nc} K_j^{AD}(T) f_j} & (\text{Re}\,action\ \ k\ \ by\ Mechanism\,1) \\ = \dfrac{1}{1+\sum_j^{nc} K_j^{AD}(T) f_j} & (\text{Re}\,action\ \ k\,by\ Mechanism\ \ 2) \\ = f_{H2} & (\text{Re}\,action\ \ k\,by\ \ Mechanism\ \ 3) \\ = \dfrac{1}{\Omega(f_{H2})\left(1+\sum_j^{nc} K_j^{AD}(T) f_j\right)} & (\text{Re}\,action\ \ k\,by\,Mechanism\ \ 4) \end{cases} \quad (11)$$

Kinetic coefficients and Langmuir coefficients can also be posed in terms of absolute temperature via Arrhenius formulae as follows:

$$\underline{K}(T) = \underline{K}_0 \bullet exp(-\underline{E}/T) \quad (12b)$$

$$\underline{K}^{AD}(T) = \underline{K}_0^{AD} \bullet exp(\underline{E}^{AD}/T) \quad (12a)$$

Component Material Balances and Numerical Resolution of Isothermal HCC

Component material balances are addressed with the vector of component molar fluxes in the reactor ($\underline{N}$), the HCC stoichiometric matrix ($\underline{\underline{H}}$), and the vector of reaction rates in Eq. (9). The resulting equation is presented below:

$$\frac{d}{dt}\underline{N} = \underline{\underline{H}}\left\{F_0\,\underline{\Psi}(T,\underline{f}) \bullet \left\{\underline{\underline{Diag}}(\underline{\underline{DK}}(T))\left\{\underline{\underline{S}}^{AD}\left(\underline{K}^{AD}(T)\bullet\underline{f}\right)+\underline{\underline{S}}^{NAD}\,\underline{f}\right\}\right\}\right\} \quad (13)$$

The numerical integration of Eq. (13), coupled to implicit algebraic resolution of Vapor-Liquid Equilibrium along the bed, leads to the determination of the effluent from the HCC reactor as follows:

$$\underline{N}^{OUT} = \underline{N}_0 + \int_{t=0}^{t=\frac{3600}{WHSV}} \underline{\underline{H}}\left\{F_0\,\underline{\Psi}(T,\underline{f}) \bullet \left\{\underline{\underline{Diag}}(\underline{\underline{DK}}(T))\left\{\underline{\underline{S}}^{AD}\left(\underline{K}^{AD}(T)\bullet\underline{f}\right)+\underline{\underline{S}}^{NAD}\,\underline{f}\right\}\right\}\right\} dt \quad (14)$$

Where *WHSV* represents the spatial velocity (kg/h/kg^{CAT}). The vector of effluent molar fluxes of all species (gmol/s) is designated by $\underline{N}^{OUT}$.

6. Parameter Estimation for the HCC Reactor Model

We used a similar strategy as done for parameter estimation of the compositional model for H-HVGO in Section 3. The available set of experimental HCC data is very similar to the set used in Section 3. Product reaction data was gathered via liquid effluent characterization from isothermal HCC runs of H-HVGO in a Pilot Plant of PETROBRAS S.A. (BRAZIL). The feed code 12 was used to mark the experiments with H-HVGO. The coordinates of HCC experiments are shown in Table 6.

In a given run, the two-phase effluent from the reactor is separated into a liquid fraction, excess H_2 and light material corresponding to paraffins with 6 or less carbon atoms. The liquid fraction was analyzed according to a routine similar to that used in Section 3 for characterization of H-HVGO. The characterization data of the liquid effluent from HCC runs is presented in da Silva (2007). In the following equations, $\underline{E}$ refers to the vector of characterizing assays for the liquid HCC product corresponding to a given temperature of reaction.

Table 6 : Experimental Coordinates for HCC

Run	*Feed Code*	*P (bar)*	*T (^oC)*	*WHSV (h^{-1})*	*H_2/Feed (NL/L)*
1	12	150.1	349.5	1.129	1654.6
2	12	150.1	359.5	1.120	1461.5
3	12	150.2	369.6	1.673	1807.2
4	12	150.1	369.4	1.120	1535.3
5	12	150.2	369.3	0.557	1886.0

The *np x 1* vector of HCC model parameters ($\underline{\hat{\theta}}$), composed by the 17 primary kinetic coefficients and 2 primary adsorption coefficients (*np=19*), was estimated for each experimental temperature by a numerical procedure as done in Section 3. The vector of model predictions for characterizing assays ($\underline{\hat{Y}}(\underline{\hat{\theta}})$) is estimated by a procedure with three steps (details can be obtained in da Silva (2007)):

- Given the run coordinates (Table 6) and the Compositional Model of the H-HVGO (Section 3), the composite feed of the reactor $\underline{N}_0$ is calculated;
- With $\underline{\hat{\theta}}$ (parameters of the reactor model) and $\underline{N}_0$, Eq. (14) is solved numerically for $\underline{N}^{OUT}$;
- After separation of residual H_2 and light hydrocarbon, $\underline{\hat{Y}}(\underline{\hat{\theta}})$ is calculated with the same methods employed in Section 3 for predicting thermodynamic properties of the liquid fraction of $\underline{N}^{OUT}$.

With $\hat{\underline{Y}}(\hat{\underline{\theta}})$, vector $\hat{\underline{\theta}}$ was optimized for each temperature according to Eq. (15) below. The weighting matrix $\underline{\underline{W}}$ is defined analogously as used in Section 3.

$$Min \ \Psi = (1/2)(\hat{\underline{Y}}(\hat{\underline{\theta}}) - \underline{E})^{t} \cdot \underline{\underline{W}} \cdot (\hat{\underline{Y}}(\hat{\underline{\theta}}) - \underline{E}) \qquad \{\underline{\theta}_L \le \hat{\underline{\theta}} \le \underline{\theta}_U\} \qquad (15)$$
$$\{\hat{\underline{\theta}}\}$$

Due to space concerns, we present in Table 7 only the estimated parameters for the HCC run at *T=349.5 ^{o}C* (HCC Run 1 in Table 6).

Table 7: Estimated Parameters ($\hat{\underline{\theta}}$) of HCC Reaction Network (*T=349.5 ^{o}C)*

Parameter	Primary Kinetic Coef.	Symbol	Value	Unit
1	1B +H	K_1	1.1E-4	mol/(s.kg^{CAT}.bar)
2	2B +H	K_2	6.6E-4	mol/(s.kg^{CAT}.bar)
3	2B –H	K_3	9.78E-5	mol/(s.kg^{CAT})
4	3B +H	K_4	8.6E-4	mol/(s.kg^{CAT}.bar)
5	3B -H	K_5	9.57E-5	mol/(s.kg^{CAT})
6	BB -C	K_6	3.79E-5	mol/(s.kg^{CAT})
7	B –R	K_7	1.61E-3	mol/(s.kg^{CAT}.bar)
8	F -R	K_8	7.6E-4	mol/(s.kg^{CAT}.bar)
9	1F -C	K_9	5.86E-6	mol/(s.kg^{CAT}.bar)
10	2F -C	K_{14}	1.18E-5	mol/(s.kg^{CAT}.bar)
11	3F -C	K_{15}	1.32E-5	mol/(s.kg^{CAT}.bar)
12	4F -C	K_{37}	2.45E-5	mol/(s.kg^{CAT}.bar)
13	5F -C	K_{65}	3.64E-5	mol/(s.kg^{CAT}.bar)
14	R12 -3C	K_{10}	1.18E-6	mol.bar/(s.kg^{CAT})
15	R24 -4C	K_{11}	4.29E-6	mol.bar/(s.kg^{CAT})
16	R24 -C	K_{12}	5.27E-7	mol/(s.kg^{CAT}.bar^2)
17	R24 -2C	K_{13}	5.17E-8	mol/(s.kg^{CAT}.bar^2)
	Primary Langmuir Coef.			
18	H_2	K_{H2}^{ADS}	8.9E-1	bar^{-1}
19	Benzene	K_{C6H6}^{ADS}	6.02	bar^{-1}

Figure 7 presents pertinent graphical results at the end of the estimation of $\hat{\underline{\theta}}$ for HCC at *T=349.5 ^{o}C.* Fig. 7A shows the Log-Log distribution of Calculated versus Experimental values (for the oil fraction). Fig 7B presents the predicted reactor profile (gmol/s) of 8H-dimethyl-Phenantrene (definetely a hydro-crackable lump). Fig. 7C displays predicted profiles of H_2 consumption for 3 classes of conversion: aromatics saturation, naphthenics cracking and hydro-conversion (i.e. dealkylation and paraffins cracking). Fig. 7D depicts predicted reactor profiles of (simulated) distillation temperatures (0.5%,5%,10%,30%, 50%, 70%, 90%, 95% and 99.5% distilled) for the oil fraction.

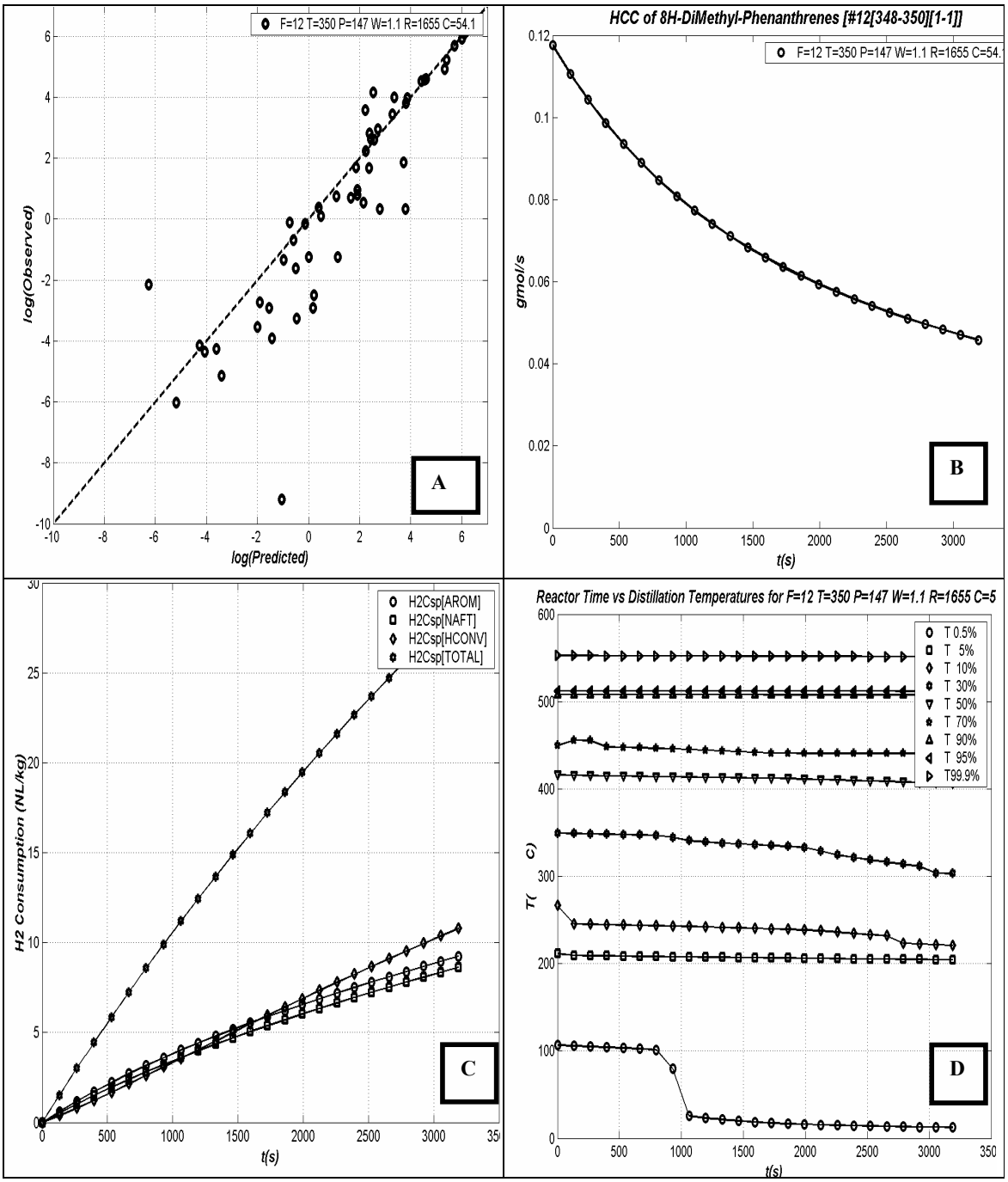

Figure 7: Results of Fitting of HCC Model at *T=349.5^{o}C* [Feed H-HVGO]
[A] log(Observed) vs log(Predicted);
[B] Reactor Profile of Lump 8H-Dimethyl-Phenantrenes *N*(gmol/s) vs *t*(s)
[C] Reactor Profiles of H_2 Consumption (NL/kg Oil) for 3 Classes of Reaction Aromatics Saturation, Naphthenics Cracking and Hydro-Conversion
[D] Reactor Profiles of % Distilled Temperatures $T_D(^{o}C)$ vs *t*(s) (for Oil Fraction)

7. Concluding Remarks

We presented a complete methodology for model development in the important field of hydrocracking (HCC) of heavy petroleum fractions. The methodology was demonstrated for a Hydrotreated Heavy Vacuum Gasoil (H-HVGO) which was studied here.

Firstly, since heavy petroleum fractions are extremely complex mixtures, any attempt of model reactive processes with these feeds needs first a consistent compositional modeling appropriate to the fraction in question. More than a composition guess, the Compositional Model is an analytical framework capable to describe accurately thermodynamic properties of the fraction, as well to establish a formal and quantitative relationship between composition transformations by the reactive process and the characterization properties of the fraction. In the present study, a compositional model was prepared for H-HVGO with molecular representatives (Lumps) pertinent to this fraction. This model was tuned with available characterization data of H-HVGO.

Secondly, in this work a useful HCC Chemical Reaction Network was proposed for the hydro-processing of feeds like H-HVGO. This network involves 235 chemical *direct* reactions, 158 species or molecular representatives (lumps), 75 kinetic rules, and 4 reaction mechanisms. It represents a compromise between the extremely high complexity of such reactive process and the necessity to achieve a valid result for engineering applications on HCC. In the present work, after the definition of the associate stoichiometric matrix, the parameter space of this network consist of all 158 component Langmuir adsorption coefficients and the 75 kinetic coefficients. In face of such large number of degrees of freedom, we opted for reducing the dimension of the independent parameter space by choosing 17 primary kinetic coefficients and 2 primary Langmuir adsorption coefficients. The remaining secondary kinetic and adsorption parameters were put as proportional to appropriate elements of the primary sets by means of pertinent information from the Literature.

Thirdly, a isothermal HCC reactor model was developed for the proposed chemical reaction network. This model neglects mass transfer resistances and radial gradients through the bed, but adopts rigorous thermodynamic equilibrium between bulk and adsorbed phases, besides continuous phase separation along the axial spatial coordinate in the reactor. Appropriate thermodynamic models for high pressure/temperature scenarios (i.e. Cubic Equations of State) were used for fugacity and vapor-liquid equilibrium calculations. All reaction rates were expressed in terms of fugacity of components and lumps according to four reaction mechanisms.

Fourthly, the remaining 17+2 parameters of the HCC reactor model were estimated via non-linear optimization to adhere the isothermal reactor model response to characterizing data of HCC products gathered with a set of HCC Pilot Plant isotermal runs. The obtained results seem reasonable and valid for engineering applications involving Hydrocracking of Hydrotreated Heavy Gasoils.

References

Barbosa, L. C., de Medeiros, J. L., Araújo, O. Q. F., Silva, da Silva R.M.C.F. (2003). Optimal Design of Lube Base Oil Hydroprocessing. *AIChE 6th Int.Conf. Refinery Proc., Proceedings, Spring Nat.Meeting*, New Orleans, USA, 26-36.

Basak, K., Sau M., Manna U., Verma, R. P. (2004). Industrial hydrocracker model based on novel continuum lumping approach for optimization in petroleum refinery. *Catalysis Today*, 98, 253-264.

da Silva, R.M.C.F. (2007). Compositional and Kinetic Modeling of Hydrocracking of Petroleum Fractions. D.Sc. Thesis. Escola de Quimica, Federal University of Rio de Janeiro (UFRJ).

de Medeiros, J. L., Barbosa, L.C., Vargas F.M., Araújo, O. Q. F., da Silva, R.M.C.F. (2004). Flowsheet Optimization of a Lubricant Base Oil Hydrotreatment Process. *Brazilian J. of Chem. Engineering, 21 (02) 317-324*.

de Medeiros, J. L., Araújo, O. Q. F., Gaspar, A.B., Silva, M.A.P., Britto, J.M. (2007). A Kinetic Model for the First Stage of PYGAS Upgrading. *Brazilian J. of Chem. Engineering, 24 (01) 119-133*.

Froment, G.F. (1987). Kinetic of the Hydroisomerization and Hydrocracking of Paraffins on Bifunctional Y-Zeolite Containing Platinum. *Catalysis Today, 1, 455-473.*

Hou, G. H., Mizan, T., Klein, M. T. (1999). Automated Molecule-Based Kinetic Modeling of Complex Processes – A hydroprocessing application. *AIChE Spring National Meeting*, Houston, TX, March 14-18.

Hydrocarbon Publishing Company – H.P.C. (2004). Advanced Hydrotreating and Hydrocracking Technologies to Produce Ultraclean Diesel Fuel (Book 1 of 2). *Hydrocarbon Publishing Company*, Southeasten, U.S.A.

Korre, S. C., Klein, M. T., Quann, R. J. (1995). Polynuclear Aromatic Hydrocarbons. 1. Experimental Reaction Pathways and Kinetics. *Ind. Eng. Chem. Res.*, 34(1), 101-117.

Korre, S. C., Klein, M. T., Quann, R. J. (1997). Hydrocracking of Polynuclear Aromatic Hydrocarbons. Development of rate Laws through Inibition Studies. *Ind. Eng. Chem. Res.*, 36(6), 2041-2050.

Martens, G.G., Marin, G.B. (2001). Kinetics for Hydrocracking Based on structural Classes: Model Development and Application. AIChE J., 47, 7, 1607-1622

Qader, S. A. (1973). Hydrocracking of Polynuclear Aromatic Hydrocarbons over Silica-Alumina Based Dual Functional Catalysts. *J. Inst. Pet.*, 59(568), 178-187.

Quann, R.J., Jaffe, S.B. (1996). Building Useful Models of Complex Reaction Systems in Petroleum Refining. *Chem.Eng. Sci.*, 51, 1615-1624.

Raychaudhuri, U., Banerjee, T. S., Ghar, R. N. (1994). Kinetic Parameters of hydroprocessing reactions in a flow reactor, *Fuel Science and Technology*, 12(2),315-333.

Reid, R.C., Prausnitz, J., Poling, B.E. (1987). *The Properties of Gases and Liquids.* McGraw-Hill, New York, USA.

Russell, C. L., Klein, M.T. (1994). Catalytic Hydrocracking Reaction Pathways, Kinetics, and Mechanisms of n-Alkylbenzenes. *Energy & Fuels*, 8(6), 1394-1401.

Svoboda, G. D., Vynckier, E., Debrabandere, B., Froment, G. F. (1995). Single-Event Rate Parameters for Paraffin Hydrocracking on a PT/US-Y Zeolite. *Ind. Eng. Chem. Res.*, Vol. 34(11), 3793-3800.

Acknowledgments

J.L. de Medeiros and O.Q.F. Araujo acknowledge research grant from CNPq, FINEP and PETROBRAS – Brazil.